Research Article | Vol. 14, No. 5 / 1 May 2024 / Optical Materials Express 1370
Optical Materials EXPRESS

Wavelength and polarisation dependence of pump-induced loss in Ti:sapphire

NIALL SIMPSON,* MARTIN LEE, AND ALAN J. KEMP

Institute of Photonics, Department of Physics, SUPA, University of Strathclyde, 99 George Street, Glasgow G1 1RD, UK
*n.simpson@strath.ac.uk

Abstract: We use pump beam wavelength and polarisation to demonstrate that the phenomenon of pump-induced loss in Ti:sapphire is linked to simultaneous excitation of two separate absorption bands: the Ti^{3+} pump band and the parasitic 400 nm residual absorption. We find that the degree of pump-induced loss is linked to the relative absorption strengths of the residual absorption band and the Ti^{3+} pump band at the wavelength(s) of excitation.

1. Introduction

Titanium-doped sapphire is a laser gain medium typically utilised for the broad gain bandwidth that enables extensive tunability and ultrashort pulse generation. The crystal's commensurately broad absorption band, however, gives rise to another type of flexibility in Ti:sapphire, namely the wide wavelength range over which the gain medium can be pumped [1]. Dye lasers, argon-ion lasers, diode-pumped solid state (DPSS) frequency-doubled YAG lasers [1] and flashlamps [2] have all been explored as Ti:sapphire pump sources. In all iterations, however, Ti:sapphire lasers are typically complex, expensive and unportable. These pumps typically limit Ti:sapphire lasers to laboratory use.

Successful diode-pumping of Ti:sapphire was first achieved in 2009 using a 1 W 450 nm diode [3], demonstrating gallium nitride (GaN) diode lasers as a potential means of achieving cheaper, more compact lasers that could be utilised by a broader scientific community. Continuing advances in laser diode technology have translated to advances in the performance of diode-pumped resonators, with an increasing range of archetypal Ti:sapphire laser performance characteristics now being achieved under diode-pumping [4]. GaN and InGaN laser diodes with >1 W output are now commercially available in the wavelength range, 445-520 nm, with the greatest output powers, ~5 W, available at the blue wavelengths (445 nm, 450 nm and 465 nm). Output powers of ~2 W are available at 490 nm, and output powers of ~1.5 W are available at 520 nm. Despite the greater powers available at shorter wavelength, many recent investigations trade higher pump power for longer-wavelength pumping, towards the more conventional 532 nm DPSSL emission. This may be partly motivated by the weaker absorption of blue wavelengths by Ti:sapphire, though, even when accounting for this reduced absorption, and higher quantum defect, unexpectedly poor performance is often reported for blue-pumped resonators [3]. Two deleterious effects have come to be associated with blue-pumping of Ti:sapphire: reduced pump fraction [5] and pump-induced loss (PIL) [3,6].

Pump fraction is the ratio of pump light absorbed by the Ti^{3+} pump absorption band relative to the total absorption; when the two-Gaussian contribution of the Ti^{3+} pump band is subtracted from the Ti:sapphire absorption spectrum, a complex residual absorption feature is identified in the 300-550 nm wavelength range, with a central wavelength ~400 nm [7]. Lower pump fraction therefore indicates a greater degree of parasitic absorption by the residual band. Blue pump wavelengths are more susceptible to lower pump fraction than "conventional" green pumps,

#511506 https://doi.org/10.1364/OME.511506
Journal © 2024 Received 10 Nov 2023; revised 20 Mar 2024; accepted 29 Mar 2024; published 24 Apr 2024

Optical Materials EXPRESS

owing to the greater overlap of pump and residual bands on the short-wavelength side of the Ti^{3+} pump band. The pump fraction also decreases with increased doping level, owing to the typical $[Ti^{3+}]^2$ dependence of the residual absorption strength [7].

In contrast to pump fraction, PIL is a dynamic effect. It was observed in the first demonstration of a diode-pumped Ti:sapphire laser, and was characterised by a degradation of resonator power with time for blue (452 nm) pumping. After a period of minutes, the laser reached a lower steady-state output power, but could be "annealed" back to the original higher power state by 532 nm pumping over several hours [3,6]. Subsequent work by Sawada *et al* has verified PIL [6], and further linked this to earlier observations of flashlamp-pumped Ti:sapphire systems made by Hoffstädt [2].

There are currently two explanations for PIL in Ti:sapphire. Sawada *et al* proposed a mechanism for PIL in which charge transfer between Ti^{3+} and Ti^{4+} ions leads to the formation of additional Ti^{3+}-Ti^{4+} ion pairs [6], with a consequent increase to Ti:sapphire's parasitic absorption at ~790 nm [8]. Studies by Moulton *et al* have provided new, detailed spectroscopic information on Ti:sapphire [7] that must be incorporated into explanations of PIL. These publications described a hitherto unreported complexity to the near-IR absorption features of Ti:sapphire that, while not dismissive of increased 790 nm absorption as the mechanism causing PIL, challenges whether additional near-IR absorption could arise directly from Ti^{3+}-Ti^{4+} pair formation. Moulton *et al.* have also suggested that the dynamic, reversible effect of PIL is consistent with the behaviour of transient colour centres found in sapphire [9]. It is apparent that further study is required to understand PIL. In light of the recent, more detailed spectroscopic characterisation of the absorption bands in Ti:sapphire by Moulton *et al.* [7], any further study must include pumping configurations that are not otherwise desirable, such as σ-polarisation pumping, and pumping with short-wavelength sources ~405 nm. More fundamentally, since little data on PIL has been acquired without co-pumping configurations that utilise multiple pump wavelengths, there is significant scope to improve understanding of the wavelength-dependence of PIL by using single-pumping arrangements.

In this paper we explore the evident wavelength-dependence of PIL in detail. By combining this with polarisation-dependence measurements, and employing a simple, quantitative means of representing the degree of loss induced in a Ti:sapphire sample, we expand significantly upon the current understanding of PIL.

Due to the current ambiguity around the origin of PIL, we conduct these experiments from a *de novo* perspective that does not rely on previous models or terminology, though we consider these models during the discussion of our results.

2. Methods

2.1. Laser resonator analysis

Data was collected by logging the 800 nm output power of a simple 3-mirror Ti:sapphire resonator cavity (Fig. 1) with a 1% transmission output coupler, under various pumping conditions. Power outputs were recorded using a Thorlabs PM100D power meter with an S121C photodiode sensor.

Beam-combining of individual diodes was achieved with dichroic mirrors suitably placed within the beam path to provide beam collinearity and spatial overlap in the Ti:sapphire crystal. Half waveplates were used at each of the diode outputs to allow polarisation control.

Though a co-pumping arrangement was employed, the pumps were (unless stated otherwise) used sequentially to (a) induce loss (at various wavelengths), then (b) anneal the crystal (at 520 nm). Each measurement thus had 2 phases; (a) loss, where the Ti:sapphire output power degrades from an initial maximum to its steady-state power and (b) annealing, where the resonator power begins at a reduced level (which we designate P_L for convenience) from the previous loss phase, but increases over time to a higher steady-state power. In each case, loss or annealing is only initiated when the preceding phase is complete. The dynamics of PIL, for example, are not

Optical Materials EXPRESS

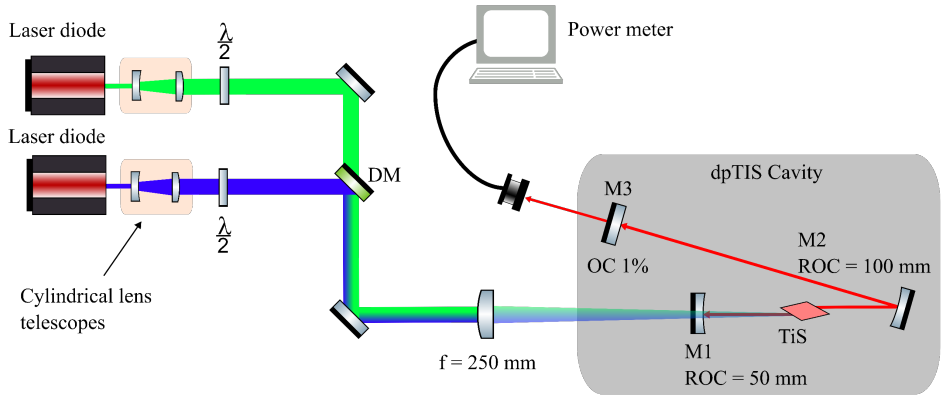

Fig. 1. Schematic diagram of the experimental setup.

observable under 450 nm-pumping if the crystal begins in a state of saturated loss. Optimisation of the cavities was performed prior to measurement, and no further optimisation was carried out during between the start of phase (a) and end of phase (b).

The following diodes were used: Nichia NDG7D75 (1.5 W @ 520 nm), Nichia NDS7175 (2 W @ 490 nm), Nichia NDB7Y7Z (5 W @ 450 nm) and Thorlabs L405G1 (1 W @ 405 nm). The stated output powers are all nominal values from the supplier; the measured powers at the crystal are referred to during discussion of the results. All diodes were collimated in the fast axis using a 4.51 mm focal length aspheric lens. Due to beam astigmatism, this lens did not fully collimate the slow axis. Cylindrical lens pairs were then employed to expand and collimate this axis. The pump beams were then focused onto the Ti:sapphire using a 250 mm focal length spherical lens. Prior to any experiments, the diode lasers were allowed to thermalise at their operating current such that stable output power was reached.

The beam size at the focus was optimised by adjusting the aspheric lens and the cylindrical lens spacing to optimise the fast axis and slow axis, respectively, while imaging and measuring the beam using a Spiricon SP620U camera. The cavity waist radii in the Ti:sapphire crystal varied between samples, and was 52 µm × 32 µm for crystal (i) 59 µm × 32 for crystal (ii), 14 × 32µm for crystal (iii) and 52 µm × 27 µm for crystal (iv). The pump spot waist radii varied with the laser diode, ranging from 22µm × 20 µm, measured for the 520 nm diode, to 59 µm × 22 µm, measured for the 450 nm diode (both in air).

2.2. Data fitting

Loss and annealing of the Ti:sapphire samples gave rise to dynamic changes in the output power. We used exponential fitting of the data to obtain a quantitative description of these processes. Multiple repetitions of loss and annealing measurements consistently yielded decay curves of bi-exponential character. Data-fitting with mono-exponential functions resulted in lower R-square values (<0.9 for loss data, < 0.97 for annealing data), while a greater number of exponential components than 2 led to redundancies in the fit. For this reason, all loss and annealing curves are treated as bi-exponential and fitted according to Eq. (1). It is likely that all data contain a contribution from long term drift of the pumps and resonator cavity, though these contributions are unlikely to be reproducible, and so cannot be accounted for. Uncertainties for the fit-parameters are determined from the standard deviation of each parameter across all

Optical Materials EXPRESS

repetitions of the experiment.

$$y = A_1 \exp\left(-\frac{x}{t_1}\right) + A_2 \exp\left(-\frac{x}{t_2}\right) + y_0 \quad (1)$$

3. Results

3.1. Application of the experimental method to 4 crystal samples

We begin this study by recording PIL from the same crystal used by Roth *et al.* [3] (crystal (i) in Table 1. Similar power-decay characteristics were observed for both PIL and annealing (Fig. 2), using a 450 nm diode to induce loss, and a 520 nm diode to anneal the crystal to its initial state. Unlike the previous studies by Roth and Sawada *et al.*, the loss phase was captured without co-pumping with green. This was performed in order to best isolate the effects of wavelength-dependence. However, utilising a single pump wavelength rather than multiple wavelengths is also crucial to the reliability of the key metric that we employ here, $L_{\%}$, as this metric is independent of pump power for a single pump, but likely becomes power-dependent with multiple pumps. The justification for this is presented during discussion of the results.

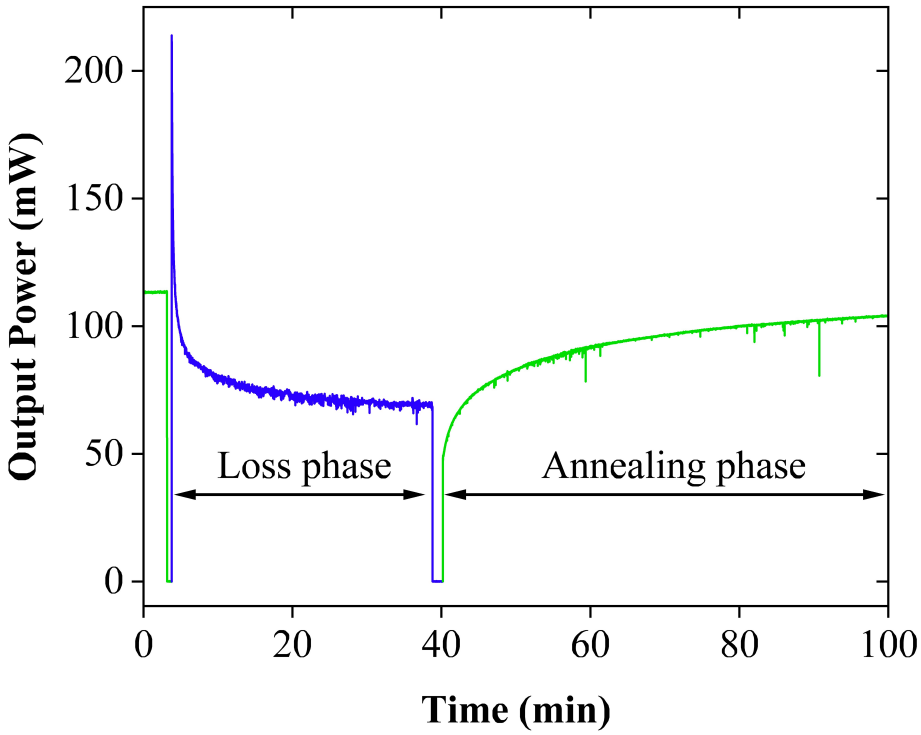

Fig. 2. Resonator output power as function of time during, initially, stable operation under green (520 nm) pumping, followed by a phase of pump-induced loss under blue (450 nm), then a phase of annealing under green pumping. Pump wavelength is represented by trace colour.

Figure 2 shows an initial period of stable output at ~113 mW under 520 nm pumping (1.4 W at diode output). Stable power verifies that the pumped volume of crystal is in an annealed state prior to the induction of loss. The green diode is then blocked and, after a short period without pumping or oscillation in the cavity, the path of a thermalised 450 nm diode is unblocked

Optical Materials EXPRESS

Table 1. List of the Ti:sapphire crystal samples investigated

Crystal	Manufacturer	Absorption coefficient, α, @ 515 nm (cm^{-1}) π-pol	Estimated absorption coefficient, α, @ 515 nm (cm^{-1}) σ-pol [1]	Growth method	Path length (mm)
(i)	St Gobain	5.3	~2.2	Czochralski	5.2
(ii)	Crystal Systems	4.8	~2.0	Heat exchange method	5.6
(iii)	Unknown	2.9	~1.2	Unknown	5
(iv)	Crystal Systems	2.37	~1.0	Heat exchange method	10

to allow pumping of the crystal. The resonator power briefly exceeds 225 mW under 4.2 W of blue pumping, but decays rapidly due to the effect of PIL. After approximately 35 minutes, the resonator power stabilises at 69 mW. This steady-state power signifies the saturation of PIL in the pumped volume of the crystal.

The blue pump is then substituted for the thermalised green pump after a period with no oscillation or pumping of the cavity. In the saturated loss state, the resonator output power has been reduced to ~48 mW under 520 nm pumping, i.e. $P_L = 48$ mW for this measurement. With continued pumping, this increases steadily, reaching 110 mW after roughly 2 hours. This gradual recovery of power demonstrates "annealing", the apparent reversal of loss, previously reported to occur at pump wavelengths of 520 nm [6] and 532 nm [3].

This figure, Fig. 2, is included to reiterate the mechanics of PIL and annealing, but also to illustrate the 2-phase experimental protocol used throughout, and to justify the subsequent method of analysis.

As reported by Roth *et al.* [3], the crystal remains in the loss state for a period of, at least, days under normal lab conditions. By translating the crystal perpendicular to the beam, the "high" power output (e.g. ~225 mW) may be recovered, though this is achieved only by pumping a volume of the crystal that has not yet been subject to loss and so begins in the "annealed" state. Translation of the crystal thus immediately leads to another loss-induction phase. For crystals (i)-(iii) PIL was consistently observed, regardless of which specific point on the crystal is pumped. It may be that there is some variation in the timescales of loss and annealing through the crystal volume due to inhomogeneities in the crystal, though that has not been investigated here. It should be noted that, in the course of this study, we determined that the most reliable way to ascertain susceptibility of a Ti:sapphire sample to PIL is to make stepwise translation of the crystal through the loss-inducing pump beam while logging the output power. As previously stated, in a sample susceptible to PIL, translation of the crystal causes an immediate switch to higher resonator output that decays; however, to distinguish this from a thermal effect it is necessary to translate the crystal back to an earlier position to check that the power remains low, indicating saturation of the PIL. Returning to the second position again will yield no further spike in the output power if the crystal is loss-susceptible.

The same experimental protocol is then applied to three additional Ti:sapphire samples, crystals (ii)-(iv) in Table 1. Using the method described above, we determined crystals (ii) and (iii) to exhibit PIL under 450 nm pumping, though for crystal (iv) we observed no deterioration of the output power with time, suggesting no susceptibility to the effect at this pump wavelength.

Figure 3(a) displays the resonator outputs under 450 nm-pumping for all 4 crystals, normalised to the initial power of the resonator in each case. Figure 3(b) shows the first hour of the corresponding annealing phases for crystals (i)-(iii) and pumping at 520nm, with the power output normalised to the level of the steady-state output. These plots are representative, showing only a single measurement; when discussing the dynamics in more detail, we refer to the values obtained by averaging over multiple repetitions of the experiment.

Optical Materials EXPRESS

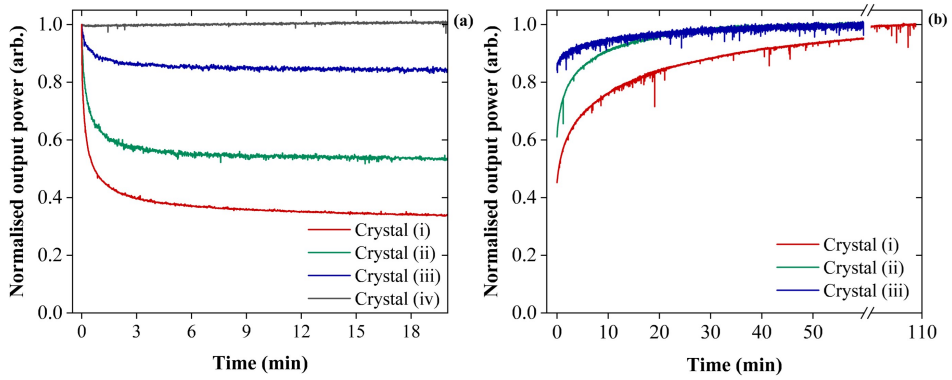

Fig. 3. Representative traces of the normalised resonator output power over time for different crystal samples during (a) pump-induced loss and (b) annealing.

Crystals (ii) and (iii) display the degradation of output power that is characteristic of PIL, though the total change in output power from peak to the stable baseline varies significantly, and in both instances is less than that of crystal (i). Crystal (iv) shows no decay in output power, and instead shows a slight increase (~1.5%) in power over the course of the measurement, possibly through thermalisation or drift in the pump power.

In Fig. 3(b), the fractional P_L (the relative output power under 520 nm pumping of the saturated loss to the fully annealed system) is lowest for crystal (i), followed by crystal (ii), then crystal (iii). This is consistent with the data taken in the loss phase, where the greatest fraction of power is lost for crystal (i) and the least for crystal (iii). Since these plots are representative single measurements, however, averaging over multiple measurements is necessary before discussing PIL or annealing quantitatively. Crystal (iv) is not present in Fig. 3(b) as there is no PIL to anneal.

We used bi-exponential fitting of the power traces to categorise the dynamics in each phase, retrieving two time-constants (t_1, t_2) and two amplitude components (A_1, A_2) for both loss and annealing. We quantify the degree of PIL by expressing the difference between P_L and the power of the fully-annealed system as a percentage of the fully annealed power. We designate this term $L_{\%}$. In this definition, $L_{\%} = 0$ when no PIL has occurred; $L_{\%}$ is higher for greater degrees of loss, indicating that P_L lies further from the output of the annealed state under 520 nm pumping. Our justification for this approach is as follows: annealing by the same π-polarised 520 nm diode is the common factor in all experiments, and the % power reduction in the green-pumped system as a result of the preceding loss-phase captures the degree of loss reasonably well. This also has the benefit of comparing the 520 nm-pumped resonator power at the two stable states of the system: the fully-annealed state and the saturated loss state.

Table 2 contains the parameters derived from exponential-fitting of the PIL data for crystals (i)-(iii). Because the $L_{\%}$ value is associated with annealing only, in Table 2 we provide an alternate parameter for loss-phase measurements; the steady-state power of the resonator in the saturated loss state, expressed as a % of the initial power level, "stable power as a % of peak" in Table 2. We consistently noted, throughout the entirety of these results, that the loss inferred through this parameter is greater than that inferred through $L_{\%}$, though we cannot provide a suitable explanation for this. This parameter is expected to be less cross-comparable between systems than the $L_{\%}$ because of the differences between diodes. Table 3 contains corresponding annealing data for each of the crystals.

The timescales quoted for loss and annealing in this study should be treated with caution and are indicative only of the general orders of magnitude, since the exact value is influenced by many factors, including: the intensity of the pump beams, the overlap of blue and green pump

Optical Materials EXPRESS

Table 2. Parameters obtained from bi-exponential fitting of the dynamics recorded during pump-induced loss for crystals (i)-(iii). The listed values are averages of the data obtained from multiple repetitions of the experiment, and the standard deviation of each value is included as the error. All PIL here was induced in π-polarisation.

Pump-induced loss							
Crystal	t_1 (s)	t_2 (s)	A_1 (mW)	A_2 (mW)	Baseline power (mW)	Maximum power (mW)	Stable power as % of peak
(i)	27 ± 5	810 ± 530	89 ± 8	30 ± 4	55 ± 18	175 ± 19	31 ± 8
(ii)	18 ± 3	180 ± 78	19 ± 2	7.8 ± 1	34 ± 1	60 ± 1	56 ± 2
(iii)	23 ± 6	1238 ± 880	7 ± 2	7 ± 4	62 ± 11	76 ± 9	81 ± 7

volumes in the crystal, the drift in both pump paths and the drift in the resonator, amongst others. The values presented here are applicable only to the conditions used in this study. We did not attempt to create a more normalised dataset by employing, for example, equal incident pump powers between diodes, or pump powers that yield equal resonator output, because the inherent differences between laser diodes create additional difficulties in this approach. For example, if we were to employ the same pump output power for all diodes then our maximum pump power is limited, by the 520 nm diode, to 1.4 W, which is below threshold for the 450 nm pump, even in π-pol. Obtaining an equivalent resonator power between different pumping conditions is even more challenging since, in these studies, the resonator output will fundamentally have two levels (P_L and the steady-state power in the annealing phase) whose separation varies by crystal and as a function of other parameters, as will be demonstrated. When varying pump wavelength, we also change absorption length, quantum defect and, as a consequence of the difference between diodes, the M^2 value of the pump. When varying wavelength and/or polarisation, we change the pump fraction. When varying the pump diode current, we also slightly change the beam size and output wavelength. It is resultantly difficult to implement conditions that allow the timescales to be discussed and compared with confidence, particularly as other wavelengths and polarisations are introduced.

We focus on the magnitude of the separation in high and low power levels that are indicative of the two stable states of the system: the fully-annealed state and the saturated loss state. Of all the diodes used in this study, the 520 nm diode has the lowest M^2 values and smallest beam size at the focus; even if the 520 nm is perfectly collinear with the other pumps used, the 520 nm pump volume will necessarily be smaller. Because we are examining the change in resonator power between the saturated-loss and annealed states, the difference in pump volumes is significant, as the 520 nm beam is only able to anneal the loss that has been induced within its volume. Therefore, in subsequent loss-phase measurements, the measured change in power level can only originate from a sub-volume of the 450 nm beam that overlaps with the smaller 520 nm volume. The signal change during loss-phase measurements is given less weight than annealing data for this reason, and it is expected that total signal change during loss-phase measurements would be larger than reported here if the 520 nm pump volume was sufficiently large to overlap with that of the 450 nm pump.

Based on these metrics, crystal (i) exhibits the greatest degree of PIL, with a $L_{\%}$ of 51 ± 2%. We also note that the degree of PIL can vary strongly by sample, from ~ 51% for crystal (i), but no loss recorded for crystal (iv). There is no apparent correlation between the growth method for these crystals and PIL. The $L_{\%}$ is seen to decrease with increasing Ti^{3+} doping level, particularly if the $L_{\%}$ for crystal (iv) is treated as 0%, suggesting that greater PIL is seen in crystals with higher doping, though confirmation of this relationship would require a larger sample set.

Optical Materials EXPRESS

3.2. Wavelength and polarisation dependence

We primarily focus on crystal (i) in our subsequent experiments where loss is induced at different wavelengths and polarisations, as the high susceptibility of this crystal to PIL allows the details of PIL to be more easily observed.

As previously, we employed a 520 nm diode as the annealing pump, in conjunction with, alternately, loss-inducing diodes with wavelengths: 405 nm, 450 nm and 490 nm. Both π (parallel to crystal c-axis) and σ (perpendicular to crystal c-axis) polarisations were examined for all wavelengths when recording PIL. Polarisation-dependence offers a means of varying the pump absorption, crucially, without altering the photon energy. The polarisation-dependence of annealing was not studied.

Figure 4(a) shows representative plots of the normalised resonator output power during the loss phase for the pump wavelengths and polarisations: σ-pol 520 nm, π-pol 490 nm, σ-pol 490 nm, π-pol 450 nm, σ-pol 450 nm. Figure 4(b) shows representative plots of the normalised power output during the corresponding annealing phases, in addition to the annealing phases for π-pol 405 nm and σ-pol 405 nm. It was not possible to measure the loss induced at 405 nm for Fig. 4(a), as the resonator could not be operated with this wavelength alone with the diode power available.

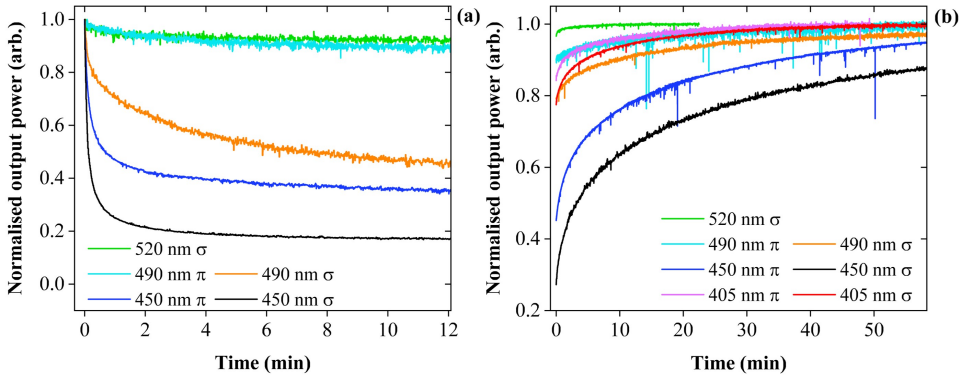

Fig. 4. Representative traces of the normalised resonator output power over time for crystal (i) during (a) PIL induced using different pump conditions (annotated) and (b) the annealing phase, carried out under 520 nm π-pol pumping. In (b), the annotations denote the pump wavelength and polarisation used to induce loss in the preceding phase.

Multiple measurements of the loss and annealing phases were performed for each studied wavelength and polarisation, and averages were taken of the parameters retrieved from bi-exponential fitting. Tables 4 and 5 contain the averaged data collected from the loss and annealing phases, respectively.

Table 3. Parameters obtained from bi-exponential fitting of the dynamics recorded during annealing, for crystals (i)-(iii)

Annealing							
Crystal	t_1 (s)	t_2 (s)	A_1 (mW)	A_2 (mW)	P_L(mW)	Steady-state power (mW)	$L_{\%}$
(i)	249 ± 63	2281 ± 568	23 ± 3	30 ± 3	50 ± 6	102 ± 9	51 ± 2
(ii)	86 ± 23	743 ± 78	8 ± 1	12 ± 1	32 ± 2	51 ± 1	38 ± 1
(iii)	79 ± 40	930 ± 414	2 ± 1	6 ± 1	53 ± 4	61 ± 4	13 ± 2

First, examining the data for 450 nm in the σ-polarisation, we see that, during the loss phase, the resonator power decreases to an average of 16 ± 3% of the peak value before reaching steady-state

Optical Materials EXPRESS

Table 4. Parameters obtained from bi-exponential fitting of the dynamics recorded during PIL, as a function of wavelength and polarisation

Pump-induced Loss							
Pump wavelength, polarisation	t_1 (s)	t_2 (s)	A_1 (mW)	A_2 (mW)	Baseline power (mW)	Maximum power (mW)	Stable power as % of peak
520 nm, σ	30 ± 7	340 ± 110	2.1 ± 0.1	1 ± 1	37 ± 1	40 ± 1	91.4 ± 0.1
490 nm, π	170 ± 22	1800 ± 600	6.1 ± 0.1	4 ± 1	76 ± 1	86 ± 1	88 ± 1
490 nm, σ	78 ± 10	750 ± 60	6 ± 1	6 ± 1	8 ± 1	20 ± 0.1	40 ± 2
450 nm, π	27 ± 5	800 ± 500	89 ± 8	30 ± 4	60 ± 20	175 ± 20	31 ± 8
450 nm, σ	10 ± 2	190 ± 30	48 ± 4	11 ± 2	12 ± 3	80 ± 15	16 ± 3

Table 5. Parameters obtained from bi-exponential fitting of the dynamics recorded during annealing, as a function of wavelength and polarisation

Annealing							
Pump wavelength, polarisation	t_1 (s)	t_2 (s)	A_1 (mW)	A_2 (mW)	P_L (mW)	Steady-state power (mW)	$L_{\%}$
520 nm, σ	19 ± 3	430 ± 120	3 ± 1	4 ± 1	190 ± 10	190 ± 10	4 ± 1
490 nm, π	150 ± 70	1750 ± 130	3 ± 1	8 ± 1	102 ± 2	113 ± 3	10.0 ± 0.1
490 nm, σ	270 ± 150	2700 ± 1600	10 ± 4	16 ± 8	70 ± 8	100 ± 11	27 ± 8
450 nm, π	250 ± 60	2300 ± 600	23 ± 3	30 ± 3	50 ± 6	102 ± 9	51 ± 2
450 nm, σ	220 ± 20	2500 ± 400	22 ± 2	31 ± 4	32 ± 4	90 ± 11	62 ± 1
405 nm π	100 ± 40	1100 ± 400	13 ± 3	15 ± 1	154 ± 1	183 ± 3	16 ± 2
405 nm σ	140 ± 50	1300 ± 600	15 ± 3	18 ± 3	153 ± 5	186 ± 1	18 ± 3

power, compared with 31 ± 8% in π-pol. The corresponding annealing data also reflects a greater degree of PIL from σ-polarised pumping; after irradiation by σ-pol 450 nm, $L_{\%} = 62 \pm 1\%$, while π-pol results in a $L_{\%}$ of 51 ± 2%.

A similar effect is observed in the loss induced by the 490nm diode, where $L_{\%}$ is 27 ± 8% after pumping with σ-pol, and 10.0 ± 0.1% after pumping with π-pol. We observed no clear polarisation dependence for 405 nm, however. In addition, the degree of loss induced at this wavelength is less than that induced at 450 nm, suggesting that a maximum degree of PIL as a function of wavelength occurs between 405-490 nm, for this sample.

It was observed that σ-pol induces greater loss than π-pol light at the same wavelength, in the range: 450-520 nm. The ability to induce a small degradation in resonator power using the 520 nm diode by rotating to σ-polarisation ($L_{\%} = 4 \pm 1\%$) is perhaps unexpected, as green wavelengths have not previously been associated with PIL. Importantly, the capacity of our annealing diode to induce loss demonstrates that both loss and annealing can occur at the same wavelength by varying the beam polarisation. This is true not only for 520 nm, but also for 490 nm and 450 nm.

Ultimately, we find that the capacity of a wavelength to induce loss or anneal the crystal is dependent on the initial state of the crystal. Again, $L_{\%}$ provides a useful reference; if we have induced loss, for example, in crystal (i) *via* π-pol 450 nm ($L_{\%} = 51\%$), annealing can be carried out with not only π-pol 520 nm ($L_{\%} = 0\%$) but also σ-pol 520 nm ($L_{\%} = 4\%$), π-pol 490 nm ($L_{\%} = 10\%$) and σ-pol 490 nm ($L_{\%} = 27\%$), despite the fact that these wavelengths and polarisations can result in PIL under alternate conditions. The *relative* $L_{\%}$ determines whether loss or annealing will occur. Following a higher $L_{\%}$ source with a lower one will anneal, but only to the limit of the annealing source, i.e. its $L_{\%}$. Inversely, if we follow irradiation using a low

Optical Materials EXPRESS

$L_{\%}$ pump with a higher one, the result is PIL. This observation encompasses the effect of both wavelength and polarisation.

It is evident that PIL arises from a photo-induced state that is not spontaneously reversible under lab conditions on the timescale of days. If we assume that the concentration of this state is higher when the loss is greater, but that annealing involves the dissociation or reversal of this state, then we can more clearly understand the ability of a single wavelength to both induce loss and anneal. Using the same example as previously, in the loss state induced by π-pol 450 nm, there is some concentration of the photo-induced state that reduces the 520 nm-pumped resonator output to 51.4% below its nominal value. Annealing by π-pol 490nm will increase the power, to a maximum of 10% below nominal output power, indicating that this wavelength will reduce the concentration of the photo-induced state but ultimately stabilise the concentration at a point where it has not been completely removed. This demonstrates that the pump wavelength is responsible for both the forward and backward rates of formation for the photo-induced state. If a clear delineation existed between a loss-wavelength or an annealing-wavelength, then we would expect loss-wavelengths to drive only a forward rate of formation, and annealing to drive only a backward rate. This would result in the same measured $L_{\%}$ for all loss-wavelengths due to a saturation of the photoproduct concentration, and $L_{\%} = 0\%$ for all annealing-wavelengths due to an absence of the photoproduct. The observation that a single pump wavelength can drive forwards and backwards rates of formation is consistent with aspects of the model of PIL proposed by Sawada *et al.* [6].

Wavelength and polarisation determine the equilibrium concentrations of the PIL photoproduct with its reactants, determining $L_{\%}$. For π-pol 520 nm pumping, we infer the lowest photoproduct concentration, followed, in order of increasing concentration by: σ-pol 520 nm, π-pol 490 nm, π-pol 405 nm σ-pol 405 nm, σ-pol 490 nm, π-pol 450 nm, σ-pol 450 nm.

It should be noted that, although we have designated $L_{\%} = 0\%$ for π-pol 520 nm, we do not have direct evidence that there is zero concentration of photoproduct in this case, only the minimum concentration studied. The significance of this will be discussed later.

As previously stated, it was not possible to capture loss-phase data from the 405 nm diode alone, owing to the negligible absorption by the Ti^{3+} pump band at this wavelength; the absorption of this wavelength in Ti:sapphire occurs primarily from the parasitic 400 nm residual absorption. Importantly, the induction of loss at 405 nm demonstrates that the mechanism of PIL is unlikely to require Ti:sapphire laser operation [6]. To resolve the dynamics of 405 nm-induced loss, we employed co-pumping of the 405 nm diode with π-pol 520 nm pump, and the results are shown in Fig. 5.

Tables 6 and 7 contain the contain the averaged data collected from the loss and annealing phases, respectively, for the 405nm diode. Unlike the previous results, the loss data here is taken through co-pumping of 405 nm (π or σ-pol) with π-pol 520 nm. The annealing, as previously, is performed with the π-pol 520 nm pump only.

Table 6. Parameters obtained from bi-exponential fitting of the dynamics recorded during PIL, as a function of the relative polarisation used in this co-pumping arrangement

Pump-induced Loss

Pump wavelength, polarisation	t_1 (s)	t_2 (s)	A_1 (mW)	A_2 (mW)	Baseline power (mW)	Maximum power (mW)	Stable power as % of peak
405 nm, π + 520 nm π	70 ± 17	1800 ± 1100	33 ± 3	8 ± 2	38 ± 6	79 ± 2	48 ± 6
405 nm, σ + 520 nm π	48 ± 5	1100 ± 200	38 ± 1	9 ± 2	25 ± 2	75 ± 6	38 ± 5

Optical Materials EXPRESS

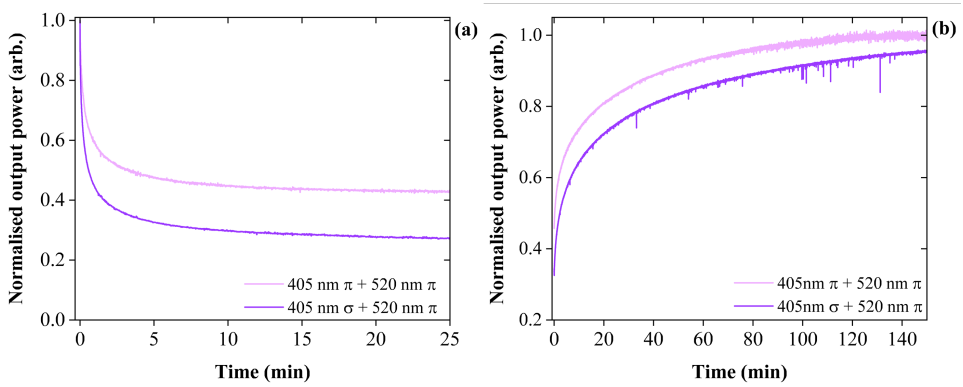

Fig. 5. Representative traces of the normalised resonator output power over time for crystal (i) during (a) PIL induced by co-pumping 520 nm with 405 nm at two polarisations (annotated) and (b) the annealing phase, carried out under 520 nm σ-pol pumping. In (b), the annotations denote the pump wavelength and polarisation used to induce loss in the preceding phase.

Table 7. Parameters obtained from bi-exponential fitting of the dynamics recorded during annealing, as a function of the relative polarisation used in this co-pumping arrangement

Annealing							
Pump wavelength, polarisation	t_1 (s)	t_2 (s)	A_1 (mW)	A_2 (mW)	P_L (mW)	Steady-state power (mW)	$L_{\%}$
405 nm, π + 520 nm π	220 ± 11	2200 ± 520	15 ± 1	26 ± 3	41 ± 2	82 ± 5	50 ± 3
405 nm, σ + 520 nm π	400 ± 120	5000 ± 1500	21 ± 3	30 ± 1	35 ± 1	84 ± 5	59 ± 1

The $L_{\%}$ values for 405 nm and 520 nm co-pumping are: 50 ± 3 for π-pol 405 nm and 59 ± 1% for σ-pol 405 nm, demonstrating that the addition of a 520 nm pump increases the degree of PIL that can be induced with a 405 nm diode.

The $L_{\%}$ values for co-pumping with these wavelengths are comparable to those obtained through 450 nm pumping. However, we must reiterate that the $L_{\%}$ of co-pumped systems is likely to be dependent on the relative power of the pumps, and comparison of the exact $L_{\%}$ from co-pumping results should also consider the absorbed power from each pump. Detailed comparison of the π-pol and σ-pol results in Table 7 is not meaningful without knowing the exact difference in absorbed 405 nm power for these crystals, which varies as result of the polarisation-dependence in: the reflection from the dichroic mirror used to combine beams, the Fresnel reflection from the Brewster-cut surface, and the Ti:sapphire absorption coefficient. We did not account for these, and so we limit our conclusion to the above statement that 520 nm increases the degree of PIL that can be induced from a 405 nm diode. Comparison to the data obtained from single-pumps is also limited for this reason.

In the course of this study we determined that laser cavity oscillation was not a prerequisite for loss or annealing to occur, with both processes occurring on similar timescales even when the resonator was blocked to prevent oscillation, suggesting that ~800 nm absorption is not required for PIL to occur. The role of 520 nm in increasing the degree of PIL obtained from the violet diode is therefore unlikely to originate from lasing in the resonator, but rather from the excitation of the Ti^{3+} pump band. Since we expect that 405 nm is absorbed only weakly into the pump band, and that π-pol 520 nm is not absorbed by the residual band, we infer this co-pumping result

Optical Materials EXPRESS

that PIL requires both excitation of the Ti^{3+} pump band and excitation of the 400 nm residual absorption.

In order to test the hypothesis that PIL originates from simultaneous excitation of the Ti^{3+} pump and residual absorption bands, we subjected crystal (iv) to 520 nm and 405 nm co-pumping. Although this sample previously showed no PIL under 450 nm pumping, we were able to induce significant loss (by ~25% of the initial output power) through a combination of 520 nm and 405 nm light. Figure 6 shows a trace of the normalised resonator output power under 520 nm-pumping, before and during irradiation with σ-pol 405 nm. There is an immediate degradation of the output power when co-pumping begins, demonstrating PIL. The absence of PIL under 450 nm pumping in crystal (iv) also supports the conclusion that PIL requires simultaneous excitation of the Ti^{3+} pump band and 400 nm residual band; because crystal (iv) is a low-doping sample and the residual band absorption strength scales as the square of $[Ti^{3+}]$, the absence of PIL under 450 nm pumping can be justified by the low absorption of the residual band at the pump wavelength in this sample; the criteria for PIL is not met. This example illustrates that the susceptibility of a crystal to PIL through 450 nm pumping alone is not-conclusive in determining whether the crystal is generally susceptible to loss.

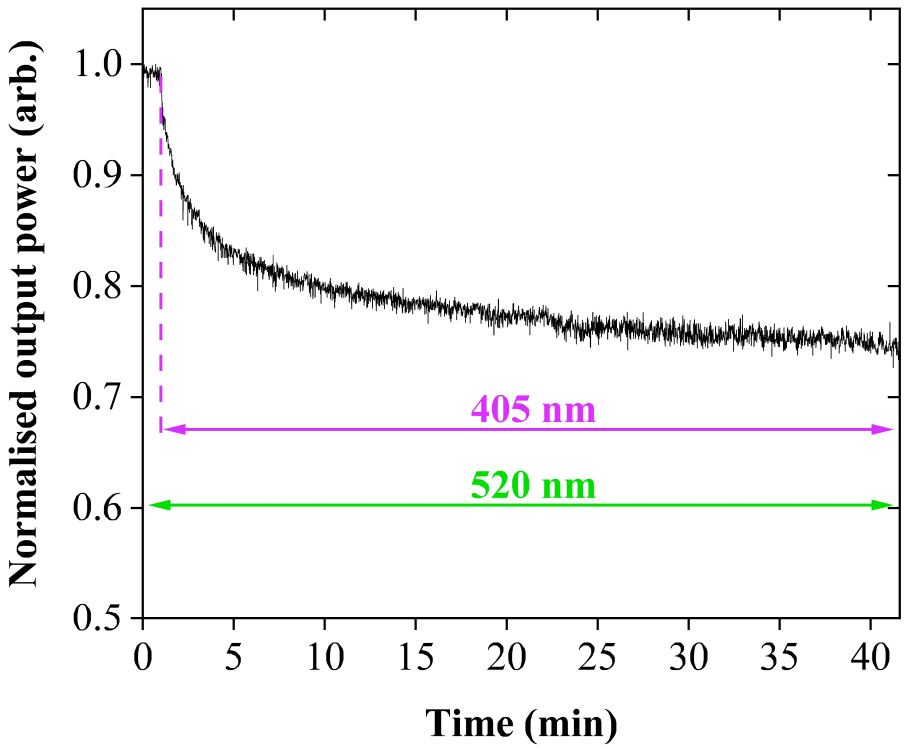

Fig. 6. Normalised output power over time for crystal (iv) under 520 nm pumping, as co-pumping with σ-pol 405 nm is initiated.

3.3. *Annealing with 405nm*

Using crystal (i), beginning in the loss state that is induced by 405 nm and 520 nm co-pumping, we observed that subsequent irradiation by 405nm light alone resulted in annealing of crystal.

Optical Materials EXPRESS

We produced a plot analogous to the previous annealing data by following the experimental steps in Table 8.

Table 8. Description of experimental protocol used to collect annealing data from 405 nm diode

Step	
1)	405 nm and 520 nm co-pumping used to saturate PIL in crystal
2)	405 nm diode used to irradiate crystal for duration, t
3)	405 nm diode switched off
4)	520 nm pumping resumes, and initial power is noted
5)	Steps (1)-(4) repeated, using different values of t

The resulting data is shown Fig. 7. The output power in this plot is normalised to the resonator output under π-pol 520 nm pumping of the fully-annealed crystal, though the system was not seen to reach this power within the measured timescale (3 hours). Data is only shown for σ-pol 405 nm annealing, owing to the longer irradiation durations studied with this polarisation. However, we observe similar annealing for the π-pol 405 nm laser.

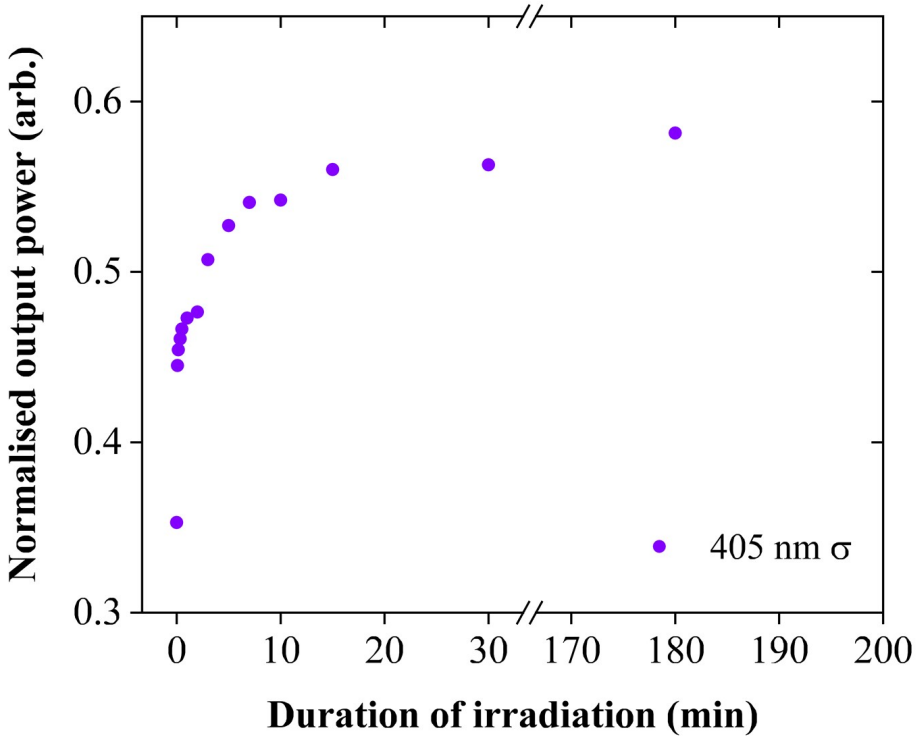

Fig. 7. Annealing of crystal (i) by irradiation with σ-pol 405 nm alone, from a loss-saturated state induced by π-pol 520nm and σ-pol 405nm pumping. The resonator power output as a function of irradiation duration is normalised to the steady-state power of the annealed, 520 nm-pumped cavity.

Because it is necessary to reset the system to its saturated loss state after the collection of each point, the data collection process for these measurements is slow, and susceptible to drift in the system power. It is nonetheless clear that annealing occurs in the sample (crystal (i)).

Optical Materials EXPRESS

After only 5 s of irradiation, the output power increases by 6.5 mW above the P_L value, an increase equivalent to 9.3% of the steady-state power. Over a period of 10 minutes, the power increases to 13.3 mW above P_L, giving a system output power that is ~54% of the steady-state output. Though longer irradiation times were measured it was observed that irradiation of 3 hours only led to a total power increase of 16 mW. The total power level at 3 hours is therefore still only ~58% of the steady-state annealed power i.e. ($L_{\%} = 42\%$). Durations longer than 3 hours were not measured, owing to the susceptibility of the measurement to drift. Ultimately, these results show that significant annealing occurs with <5 s of irradiation. After ~10 minutes of irradiation, the annealing rate is much slower. From our previous observations, we expect that each wavelength/polarisation can anneal PIL to a limit determined by the P_L of the source. In this case we thus expect that σ-pol 405 nm can anneal the crystal to ~80% of the full resonator power ($L_{\%} = 18 \pm 3\%$), however, this does not occur within the measurement period.

4. Discussion

Taken together, these experimental results support the conclusion that PIL involves both the residual absorption band and Ti^{3+} pump band. When excitation of these bands occurs together, which is possible across a broad range of blue-green pump wavelengths, it results in a photoproduct that increases loss in the gain medium. Individually, however, each excitation can result in dissociation of the photoproduct, i.e. annealing. These processes can broadly be represented with the following expressions:

$$m(\mathrm{Ti}^{3+} + h\nu_{\mathrm{Ti}^{3+}}) + n(\mathrm{R} + h\nu_{\mathrm{R}}) \rightarrow \text{Photoproduct} \qquad \text{PIL}$$

$$\text{Photoproduct} + h\nu_{\mathrm{Ti}^{3+}} \rightarrow m\mathrm{Ti}^{3+} + n\mathrm{R} \qquad \text{Annealing (green)}$$

$$\text{Photoproduct} + h\nu_{\mathrm{R}} \rightarrow m\mathrm{Ti}^{3+} + n\mathrm{R} \qquad \text{Annealing (violet)}$$

Where R denotes the chemical species in the residual band that is excited to form the loss-inducing photoproduct, $h\nu_{\mathrm{Ti}^{3+}}$ and $h\nu_{\mathrm{R}}$ denote photons absorbed by Ti^{3+} and R, respectively, and m and n denote integers that satisfy the stoichiometry requirement for the reaction. These expressions make apparent that a single wavelength that is absorbed both by Ti^{3+} and R will participate in both the loss and annealing processes. When PIL occurs, the photon energies required to form the loss-inducing photoproduct are also able to anneal this photoproduct. From this, a dynamic equilibrium is established between the loss-inducing photoproduct and its reactants, the Ti^{3+} and the residual-band subcomponent, R. It should be noted, from [7], that R is likely to be a Ti^{3+} ion pair.

Our results suggest that the concentration of photoproduct at equilibrium (equivalent to the saturated loss state, ~ $L_{\%}$) is determined by the relative absorption strengths of the pump and residual bands, at the wavelength and polarisation of the pump. We now consider this quantitatively.

Figure 8 shows the residual absorption band of crystal (i), in π-polarisation, obtained through subtraction of the pump band absorption, as described in [7]. The pump band fit is included for reference, and pump wavelengths are annotated on the plot as dashed lines, allowing visualisation of the relative absorption strengths of both pump and residual bands at the various wavelengths used in this study.

In the Ti:sapphire absorption spectrum, the pump band absorption peaks ~490 nm, and the residual absorption peaks ~ 400 nm; in the ~100 nm region of overlap between these absorbances, the ratio of residual absorption to pump band absorption is closest to unity at 434 nm. Either side of 434 nm, a pump wavelength will increasingly interact more strongly with one band than the other. To quantify this, we define an absorption ratio as the stronger absorption coefficient divided by the weaker absorption coefficient. This quantity increases from unity in proportion to the degree to which a particular pump wavelength excites one band more strongly than the other.

Optical Materials EXPRESS

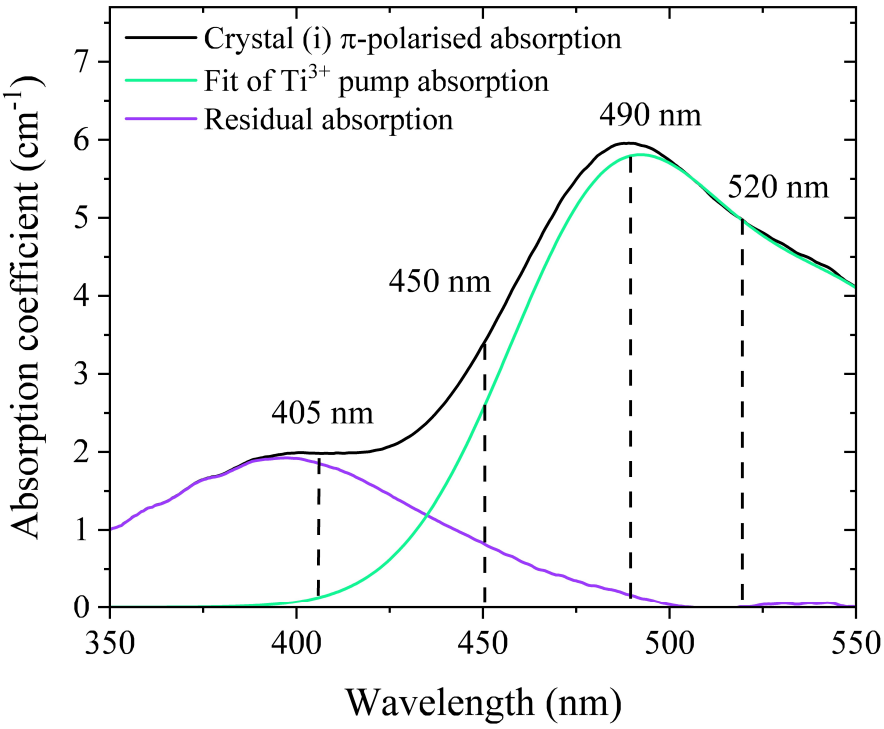

Fig. 8. The absorption spectrum of crystal (i) in π-polarisation (black), alongside the fit of the pump band absorption (green), and the resulting residual absorption (purple) with dashed lines to indicate where the diode wavelengths intersect with the spectra.

At 405 nm and 490 nm, the diode wavelengths are each strongly absorbed into one band, and weakly absorbed into the other. At 490 nm the absorption ratio is 31 and the $L_{\%} = 10\%$. At 405 nm, the absorption ratio ($\alpha_{residual}$ to α_{pump}) is 15, and the $L_{\%} = 16\%$. When the ratio of absorptions is smaller, a greater degree of loss is observed; our highest degree of PIL ($L_{\%} = 51\%$) occurs for 450 nm pumping, where the ratio of α_{pump} to $\alpha_{residual}$ is 3.

A comparable degree of loss ($L_{\%} = 50\%$) is observed for co-pumping with 405 nm and 520 nm. Though it is unintuitive to expect greater PIL from a 405 nm diode by combining this with a source that only leads to annealing, the result can be justified by considering the absorption ratios at the positions of each pump wavelength; the ratio of α_{pump} at 520 nm with $\alpha_{residual}$ at 405 nm is 2.7.

A similar deconvolution of pump and residual bands can be applied to crystals (ii)-(iv), and to crystal (i) in σ-pol. If we then assume the pump wavelength and polarisation only significant insofar as they change the absorption ratio of the pump, and similarly, we assume the differences between crystals are significant only because the absorption band ratios may change as consequence of doping, then we can combine and compare nearly all $L_{\%}$ values measured here as a function of only the corresponding ratio of the pump band and residual band absorption strength. The result is the plot shown in Fig. 9.

Though more data points are required, preferably from a variety of crystal samples, Fig. 9 begins to demonstrate a relationship between PIL and the band ratio. With decreasing ratio, i.e. more comparable intensity between the pump and residual bands, $L_{\%}$ increases. This relationship may be due to the stoichiometry of product formation, with product formation becoming most

Optical Materials EXPRESS

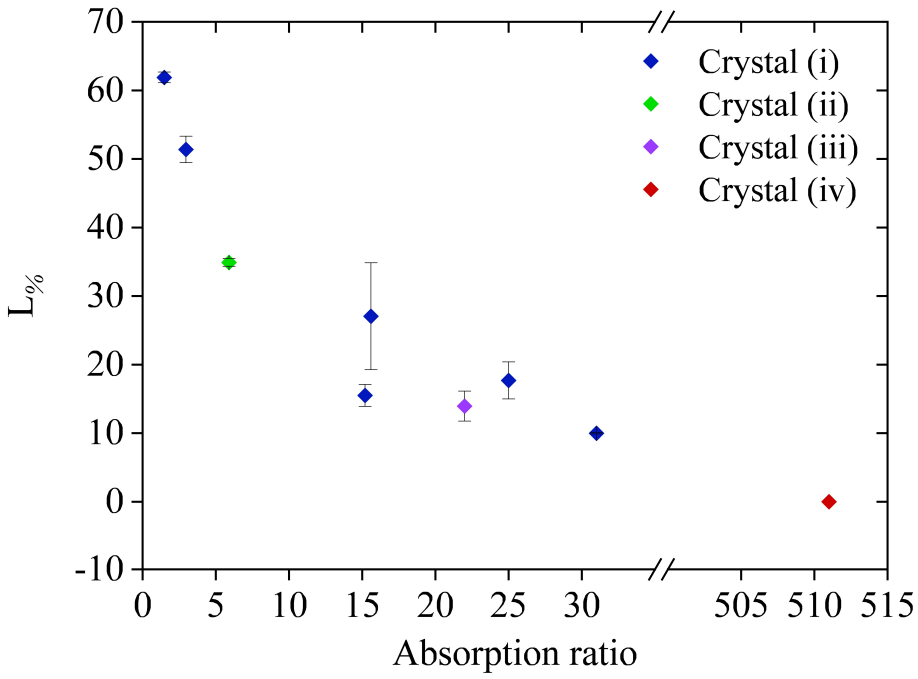

Fig. 9. $L_{\%}$ as a function of the ratio of absorption ratio (stronger band/weaker band) for all crystals, and all wavelengths and polarisations of crystal (i), excluding π-pol 520 nm. The $L_{\%}$ of crystals (ii) and (iii) in Fig. 9 have been scaled for a crystal of path length 5.2 mm

likely to occur when stoichiometric quantities of the excited-state reactants are present. A maximum degree of loss at an absorption ratio of ~1 seems unlikely from this, however, as the equivalence between absorption strength and the number of excited-state reactants is a function of both the oscillator strength for each absorption as well as the excited-state lifetime for the species. It seems more likely that the increase in loss as the absorption ratio approaches 1 is a consequence of the photon stoichiometry; at anything other than a 1:1 ratio of $hv_{Ti^{3+}}$ and hv_R, there will be an excess of one photon species that will make annealing more favourable.

Further information is required to interpret the trend of Fig. 9 in more detail. However, we can infer that the wavelength and polarisation dependences of PIL are a consequence of the changing absorption ratio with wavelength. Further, the apparent increase in $L_{\%}$ with higher crystal doping can also be explained as consequence of the changing absorption ratio. Studies by Moulton *et al.* have shown that the residual band absorption strength scales as the square of Ti^{3+} doping; because the relative absorption strengths of pump and residual band is not constant with doping, at a fixed wavelength, for example ~450 nm, an increase of the doping level would increase to α_{pump} which in turn would, broadly, be expected to increase $L_{\%}$. In crystal (iv) no PIL was observed under 450 nm pumping, which we suggested was due to the lack of residual-band excitation. For this sample, the strength of the Ti^{3+} absorption is a factor of ~500 greater than that of the residual band, supporting this explanation.

It should be noted when comparing different crystals, however, that the metric, $L_{\%}$, is likely to vary with the crystal length. It has been proposed that PIL leads to an increase in the parasitic NIR absorption of Ti:sapphire [6], in which case the total loss is expected to follow Beer's Law, where an increase in path length increases the total absorption. To account for this, the $L_{\%}$ of crystals (ii) and (iii) in Fig. 9 have been scaled for a crystal of path length 5.2 mm, i.e. to the

Optical Materials EXPRESS

same length as crystal (i). It should be noted that the resulting difference to $L_{‰}$ is very small owing the similar path lengths of these crystals.

We have omitted three results from Fig. 9: σ-pol 520 nm, and the two co-pumping results. In the σ-pol 520 nm measurement, the band ratio was 6.9, from which we would expect a significantly larger $L_{‰}$ than measured (3.5‰). We justify the omission by way of a set of earlier studies of the fluorescent properties of Ti:sapphire crystals, in which we identified a subset of our samples that exhibited a sharp emission line ~ 693 nm, with two weaker emission peaks at ~ 669 nm and 716 nm. The fluorophore was identified as a Cr^{3+} impurity through fluorescent lifetime measurements; we measured a lifetime of ~3.2 ms for the 693 nm peak [10]. From this, the Ti:sapphire absorption of some samples is convoluted with that of Cr^{3+}. We identified Cr^{3+} impurity in crystal (i), and thus expect additional absorption bands at ~400 nm and ~550 nm in this sample. The 550 nm absorption band of Cr^{3+} is strongly polarisation-dependent, with stronger absorption in σ-pol [11], and we find in crystal (i) that a peak is observed ~ 550 nm in the σ-pol residual spectrum that is not well-defined in π-pol. We thus propose that the low band ratio for σ-pol 520 nm may be a consequence of the underlying Cr^{3+} absorption at this wavelength.

The induction of loss at σ-pol 520 nm can, however, be explained by work from Moulton et al. [7], as this study demonstrates that the residual band extends to longer wavelengths in σ-pol. From this, σ-pol 520 nm is able to simultaneously excite both the residual and pump bands, though with a high band ratio that gives a low, but nonzero, $L_{‰}$.

From π-pol to σ-pol, the Ti^{3+} pump band absorption strength decreases significantly, while the residual band absorption strength changes comparatively little. From this, the absorption ratio in σ-pol is generally smaller, giving rise to higher $L_{‰}$. We acknowledge a possible inconsistency regarding polarisation-dependence in the of 405 nm and 520 nm co-pumped system, however. In altering the 405 nm polarisation from π- pol to σ-pol we observe greater $L_{‰}$, though no change to the absorption ratio has occurred at either 405 nm or 520 nm. However. it has been shown that, in a co-pumping configuration, the degree of PIL is affected by the absorbed power of the pumps [6]. The polarisation-dependence in this co-pumping result may therefore reflect a difference in absorbed power.

We now use the expressions set out at the beginning of the section to provide justification for our assertion that $L_{‰}$ is independent of pump power for a system with only one pump, but becomes dependent on pump power in a co-pumped system. As discussed, for PIL to occur, there must be pump photons absorbed by both the Ti^{3+} pump band and the residual band. When these absorption bands spectrally overlap, there is a resulting overlap in the energies of $h\nu_{Ti^{3+}}$ and $h\nu_{R}$, such that a single pump wavelength can provide both $h\nu_{Ti^{3+}}$ and $h\nu_{R}$, resulting in PIL. In this case, the number of absorbed $h\nu_{Ti^{3+}}$ photons relative to absorbed $h\nu_{R}$ photons ($h\nu_{Ti^{3+}}$: $h\nu_{R}$) is dependent only on the relative absorption coefficients of the two bands at the pump wavelength. The relative absorption, or the absorption ratio, determines $L_{‰}$. If the pump power increases, $h\nu_{Ti^{3+}}$: $h\nu_{R}$ remains constant because the relative absorption coefficients are also constant, hence $L_{‰}$ does not change.

In a co-pumped system with more than one pump wavelength, each wavelength has a fixed, but different, value of $h\nu_{Ti^{3+}}$: $h\nu_{R}$, and $L_{‰}$ is determined by considering $h\nu_{Ti^{3+}}$: $h\nu_{R}$ for the *combined* beam. This is supported by the data in Figures (5) and (6). If the power of one pump in this configuration is changed while the other pump powers remain constant, the number of absorbed photons increases at one wavelength. Because $h\nu_{Ti^{3+}}$: $h\nu_{R}$ is different between wavelengths, the $h\nu_{Ti^{3+}}$: $h\nu_{R}$ for the combined beam changes with power level, changing $L_{‰}$. From this, the pump powers of a co-pumped system should be expected to provide a weighting to PIL or annealing. This is consistent with observations by Sawada *et al.* who have demonstrated that the equilibrium power level of a resonator co-pumped with 520 nm and 451 nm decreases as the power of the 451 nm is increased [6], i.e. the $L_{‰}$ increases as the absorbed 451 nm power increase.

Optical Materials EXPRESS

Throughout this discussion we have referred to the 400 nm residual absorption band as the source of one of the excitations giving rise to PIL. We must acknowledge that the residual band is a complex set of absorption features that does not arise from a single contribution, and whose composition may vary from crystal to crystal with impurities or defects. Ti^{3+} ion pairs form the most significant contribution to the 400 nm residual band [7], but we cannot exclude the possibility that PIL is related to another sub-component of the band. In the case that PIL is linked to point defects or impurities with a broad absorption features in the ~400-490 nm wavelength range, it might be expected that the susceptibility of PIL varies from crystal to crystal, and that some crystals simply do not exhibit PIL. In the case that PIL arises from Ti^{3+} pair absorption, however, we expect PIL to be possible in any Ti:sapphire crystal, though to different extents determined primarily by the Ti^{3+} concentration. Since we have observed that the PIL in our samples is linked to the pump band absorption coefficient, our experimental results appear to favour the explanation that PIL is related to Ti^{3+} pairs.

Our results support aspects of the model proposed by Sawada *et al*. [6], specifically the dual-role of certain wavelengths in both loss-induction and annealing. Our results do not allow us to confirm or discount other aspects of the model, however, such as the increase in parasitic absorption at 800 nm being the mechanism causing PIL. Further, our observations that laser oscillation is not required for loss or annealing to take place does not support the Ti^{3+}-Ti^{4+} charge-transfer model, in which absorption of 800 nm photons is posited to excite Ti^{4+} from the ground to excited state as a prerequisite step to charge-transfer. Similarly, our observation that PIL requires excitation of the Ti^{3+} pump band does not support the hypothesis by Moulton *et al*. that PIL originates from colour centres unrelated to the Ti^{3+} ion [5].

In this study we have treated the annealed state under π-pol 520 nm pumping as having $L_{\%} = 0\%$, i.e. that the concentration of the loss photoproduct is zero. Without a longer pump wavelength as reference, it cannot be determined experimentally whether this is true. From the work of Moulton *et al*. [7], it is reasonable to assume that that the residual absorption band only extends as far as 500 nm in π -pol, and that no PIL occurs for π-pol 520 nm. An interesting implication of this, however, is that PIL may be difficult to verify with only one pump wavelength available.

It was previously suggested that longer wavelength pumps are more desirable for diode-pumped Ti:sapphire resonators, in part due to the effect of pump fraction [5]. While the additional information on PIL presented here may seem to reinforce this conclusion, we add two caveats: (i) when the Ti^{3+} doping becomes sufficiently high, pump fraction and PIL become a consideration even at longer wavelengths such as 490 nm, and perhaps even 520 nm, and (ii) when the Ti^{3+} doping is sufficiently low, the effects of pump fraction and PIL become negligible, allowing the use of cheaper, shorter-wavelength, higher-power diode pumps without these deleterious effects.

Reliance on longer-wavelength diode-pumps to circumvent these effects may not be sufficient where multiple pumps wavelengths are combined using dichroic mirrors, particularly if wavelengths such as 465 nm and 490 nm are used, since these may still give rise to PIL in some crystals. Strategies such as polarisation beam-combining, or beam-combining through an optical fibre in which polarisation is not preserved, may also be less viable than predicted due to the polarisation-sensitivity of PIL.

Further study is required to fully expand upon the work here. A technique such as EPR spectroscopy [12], for example, may be able to identify and characterise the photoproduct that gives rise to PIL. It has also been proposed that the PIL photoproduct increases cavity loss through an increase of the 800 nm parasitic absorption in Ti:sapphire [6]. This is difficult to study spectroscopically, since the changes are very small, but intracavity absorption spectroscopy may be a viable approach. Another spectroscopic investigation of potential significance to PIL would be a time-resolved UV-Vis study that probes the interaction between the residual absorption band and Ti^{3+} pump band. It seems possible from steady-state spectroscopic data that the Ti^{3+}

Optical Materials EXPRESS

and Ti^{3+}-Ti^{3+} absorptions do not originate from mutually-exclusive populations of Ti^{3+} ions, i.e. that clustered Ti^{3+} ions are in a dynamic equilibrium between the Ti^{3+}-Ti^{3+} and $2Ti^{3+}$ states. A time-resolved technique may be able to probe the exchanges between these populations.

It is interesting to speculate on how the relation in absorption strength could be explored to yield additional quantitative information on PIL. For example, if we were to combine a pump close to the centre wavelength of the residual band, such as 405 nm, with a second pump that is only weakly absorbed at the short-wavelength edge of the pump band, it may be possible to maximise the PIL in such a way as to saturate the photoproduct concentration in the sample. This would allow the limits of PIL to be explored from crystal to crystal, and perhaps related to the ion concentrations of the samples to yield stoichiometric information on the photoproduct formation.

The root cause of both PIL and pump fraction may be the formation of Ti^{3+} ion pairs in Ti:sapphire [7]. Investigations into alternate growth or annealing processes that can still effectively reduce parasitic near-IR absorption while limiting the formation of $[Ti^{3+}]^2$ could yield interesting Ti:sapphire samples to analyse from the standpoint of both PIL and pump fraction.

5. Conclusion

We have demonstrated that PIL requires excitation of both the Ti^{3+} and the 400 nm residual band to occur simultaneously. Due to the overlap of these two absorption bands, simultaneous excitation is possible at a single wavelength, though the same effect can be produced using two separate wavelengths. Individually, the excitations result in annealing of PIL. The degree of loss induced is linked to the relative absorption strengths of the residual band and the Ti^{3+} pump band at the wavelength, or wavelengths, of excitation, with lower absorption ratios, approximately ~1, giving rise to greater PIL. The relative absorption strength can also be altered *via* polarisation control, giving rise to a greater degree of PIL in σ compared to π-pol. Due to the dependence of residual band absorption strength on $[Ti^{3+}]$ we expect greater susceptibility PIL in highly doped crystals. We propose that future power-scaling of diode-pumped Ti:sapphire systems must balance these considerations for the most effective utility of the diode pumps available. Further investigations of PIL are suggested, as a means of better understanding the effect in order to mitigate it.

Funding. Engineering and Physical Sciences Research Council (EP/T014288/1).

Acknowledgements. We acknowledge Milan Adelt and Daniel Doveiko from the Photophysics Group at the University of Strathclyde, and Anna Gakamsky of Edinburgh Instruments, for their expertise in performing fluorescence measurements.

Disclosures. The authors declare no conflict of interest.

Data availability. Data underlying the results presented in this paper are available from the University of Strathclyde data repository [13].

References

1. P. F. Moulton, "Spectroscopic and laser characteristics of Ti:Al_2O_3," J. Opt. Soc. Am. B **3**(1), 125 (1986).
2. A. Hoffstadt, "High-average-power flash-lamp-pumped Ti:sapphire laser," Opt. Lett. **19**(19), 1523 (1994).
3. P. W. Roth, A. J. Maclean, D. Burns, *et al.*, "Directly diode-laser-pumped Ti:sapphire laser," Opt. Lett. **34**(21), 3334–3336 (2009).
4. H. Liu, S. Sun, L. Zheng, *et al.*, "Review of laser-diode pumped Ti:sapphire laser," Microw. Opt. Technol. Lett **63**(8), 2135–2144 (2021).
5. P. F. Moulton, J. G. Cederberg, K. T. Stevens, *et al.*, "Optimized InGaN-diode pumping of Ti:sapphire crystals," Opt. Mater. Express **9**(5), 2131 (2019).
6. R. Sawada, H. Tanaka, N. Sugiyama, *et al.*, "Wavelength-multiplexed pumping with 478- and 520-nm indium gallium nitride laser diodes for Ti:sapphire laser," Appl. Opt. **56**(6), 1654 (2017).
7. P. F. Moulton, J. G. Cederberg, K. T. Stevens, *et al.*, "Characterization of absorption bands in Ti:sapphire crystals," Opt. Mater. Express **9**(5), 2216 (2019).
8. R. L. Aggarwal, A. Sanchez, M. M. Stuppi, *et al.*, "Residual Infrared Absorption in As-Grown and Annealed Crystals of Ti:Al_2O_3," IEEE J. Quantum Electron. **24**(6), 1003–1008 (1988).

Optical Materials EXPRESS

9. B. D. Evans and L. S. Cain, "A cation vacancy center in crystalline Al_2O_3," Radiat. Eff. and Defects in Solids **134**(1-4), 329–332 (1995).
10. T. H. Maiman, R. H. Hoskins, I. J. D'Haenens, *et al.*, "Stimulated Optical Emission in Fluorescent Solids. II. Spectroscopy and Stimulated Emission in Ruby," Phys. Rev. **123**(4), 1151–1157 (1961).
11. C. Song, Y. Hang, C. Xia, *et al.*, "Characteristics of large-sized ruby crystal grown by temperature gradient technique," Opt. Mater. **27**(4), 699–703 (2005).
12. B. W. Faughnan and Z. J. Kiss, "Photoinduced Reversible Charge-Transfer Processes in Transition-Metal-Doped Single-Crystal $SrTiO_3$ and TiO_2," Phys. Rev. Lett. **21**(18), 1331–1334 (1968).
13. N. Simpson, M. Lee, and A. J. Kemp, "Wavelength and polarisation dependence of pump-induced loss in Ti:sapphire: data," University of Strathclyde, 2024, https://doi.org/10.15129/2f961873-113c-4136-b732-1c7a80aff4ab.